THE JOURNAL OF PHYSICAL CHEMISTRY C

C: Energy Conversion and Storage; Energy and Charge Transport

Triplet Excited State Energetics and Dynamics in Molecular "Roller Wheels"

Maksim Y. Livshits, Wenhan He, Zhen Zhang, Yang Qin, and Jeffrey J. Rack

J. Phys. Chem. C, **Just Accepted Manuscript** • DOI: 10.1021/acs.jpcc.9b03934 • Publication Date (Web): 11 Jun 2019

Triplet Excited State Energetics and Dynamics in Molecular "Roller Wheels"

Maksim Y. Livshits, Wenhan He, Zhen Zhang, Yang Qin,* and Jeffrey J. Rack*

Department of Chemistry & Chemical Biology, University of New Mexico, Albuquerque, NM 87131.

ABSTRACT: We report the photoinduced excited state dynamics of a series of novel Pt(II)-bisacetylide containing conjugated small molecules that possess geometric shapes resembling "roller wheels," but differ in lengths of the linear conjugated chromophores, *i.e.* the "rollers". We measure excited state evolution and triplet formation by ultrafast pump probe transient absorption followed by quantifying the triplet decay lifetimes using nanosecond flash photolysis transient absorption techniques. Two of these complexes of relatively longer chromophore lengths and smaller bandgaps do not show phosphorescence emission. Thus, the triplet energy is approximated by quenching, utilizing fullerene derivatives with varying lowest unoccupied molecular orbital (LUMO) energies. Furthermore, $^3O_2$ quenching experiments are performed in order to quantify the minimum triplet excited state quantum yields for these complexes. Lastly, our fullerene and $^3O_2$ transient absorption quenching data demonstrate that the estimations of excited state energies by cyclic voltammetry is not always accurate for these low band-gap organic materials, which require more extensive photophysical studies.

INTRODUCTION

The rapid development of organic electronics, including organic light emitting devices (OLEDs)[1] and organic photovoltaics (OPVs),[2-4] in the past several decades has been propelled by the development of new material structural designs, and progress in understanding structure-property-function relationships. Such relationships include the impact of molecular architecture on exciton multiplicity, energetics, dynamics and performance. In particular, both short-lived singlet and long-lived triplet excitons can be generated in organic materials upon light absorption or charge injection. The use of triplet states in OPVs are much less explored relative to singlet excited states, in part because triplets have been shown to either improve or decrease device performance, depending upon experimental conditions. Triplet "scrubs" have been shown to enhance OPV performance of P3HT:PCBM blends by trapping triplet exciton, before they can influence surrounding P3HT:PCBM charge separated states to produce more triplets rather than free charges.[5] Meanwhile, other materials exhibiting triplets benefit from longer triplet diffusion lengths (relative to singlet exciton) as well as forbidden geminate recombination (if intersystem crossing (ISC) takes place in the charge separated state before creation of free charges), thus, in principle leading to more efficient charge separation and diffusion.[5-9] However, in the event a singlet fission mechanism is operative (within the single junction device), the theoretical efficiency of an organic singlet fission material energy transfer into the bulk semiconductor is calculated to be around 50%, surpassing the well-known Shockley-Queisser limit at ca. 33%.[10] This possibility has driven much of the development of triplet exciton materials. Thus, understanding the production and fate of triplet excitons in materials with designed chemical structures is critical to advancement of OPVs.

Much of the attention in the design of triplet generating OPV materials has been focused on triplet sensitization of conjugated polymers utilizing doped or pendant chromophores (organic $n \rightarrow \pi^*$ or transition metals).[11-12] Other strategies of directly generating triplet excitons within pure OPV organic structure involves combinations of electron-rich and electron-poor units in alternating fashion, with a covalently attached heavy metal atom (ion) for enhanced intersystem crossing (ISC).[5, 13-19] The best researched strategies are generated from push-pull organometallic platinum-bisacetylide-containing polymers and small molecules in OPVs and OLEDs, where two sterically bulky platinum-bisacetylide moieties are placed at both ends of a linear multi-aromatic organic chromophore, forming structures resembling that of "dumbbells".[12, 20-21] Extensive studies on this type of materials have revealed how structural changes can alter the bandgap, morphology, triplet exciton dynamics and device performance. The results of such studies have produced OLEDs with tunable emission over the visible range as well as OPVs with efficiencies of ca. 1-2%. It has also been demonstrated by transient absorption and quenching studies that triplet excitons can possess long diffusion lengths as well as be split into free charges at the donor-acceptor interfaces.[7, 21-22]

Further experimentation of these dumbbell structures and polymers did in fact reveal a series of unintended consequences. Even with near unity ISC from the singlet to a long lived triplet excited state (>1 μs), incorporation of the platinum-bisacetylide units along the backbone of the polymer introduces steric stress, thus lowering the crystallinity of the material.[21-22] The amorphous nature of these polymers, presumably due to the large volume of the platinum complexes, decreases π−π stacking between the polymer backbones, thus inhibiting necessary interchromophore diffusion of charges and excitons. More recent work has demonstrated that relocating single strand "push-pull" organometallic platinum-bisacetylide units to the side chains of an insulating polymer yields wide gap polymers(~2.9 ev) with near unity energy transfer efficiency up to 300 repeat units.[23]

Previously, we reported a series of "roller wheel" type platinum-bisacetylide donor-acceptor architectures (**RWPt**), which exhibit much improved OPV device performance of up to ca. 6% power conversion efficiency (PCE) and long lived triplet excited states of lifetimes up to 14 μs.[24-25] In contrast to the "dumbbell" type architecture, the new "roller wheel" like structure positions the platinum in the center of the linear organic chromophore as side chains. This synthetic modification has led to an increased power conversion efficiency, which is ascribed to a slip stack semi-crystalline morphology enabling better charge mobility from π–π stacking.[25] Interestingly, our initial studies demonstrated by nanosecond flash photolysis and computational analysis that the long lived triplet excited state is too low in energy to be quenched by phenyl-C_{61}-butyric acid methyl ester (PCBM), thus unequivocally showing that OPV performance originates from PCBM quenching of the RWPt singlet excited state. Henceforth, photophysical studies on the RWPt platform along with quencher screening to experimentally approximate the triplet energy is imperative to advance our understanding of RWPt (donor) fullerene (acceptor) interactions. Once capture of the triplet excitons can be demonstrated, it will be possible to measure important properties such as the triplet diffusion length, mechanism of energy transport and efficiency of triplet exciton splitting at the interface, all of which are important factors for advancing the field of triplet OPV devices.

Herein, we present our first series of findings examining the structure function relationship leading to triplet generation in the RWPt compounds as well as approximating the triplet energy by screening a series of fullerene derivative quenchers including $^3O_2$. As mentioned above, we have previously published that PCBM does not capture triplets in **RWPt-1** and **RWPt-2**; therefore, unfunctionalized C60 and a cationic fullerene with descending LUMO energies are investigated as quenchers. The impact of the arm length on the triplet generation is correlated by pump probe transient absorption studies, which give us useful insights on future improvement of such materials in optoelectronic devices.

EXPERIMENTAL SECTION

All reagents and solvents were used as received from Sigma-Aldrich or WVR unless otherwise noted. Phenyl-C61-butyric acid methyl ester (PCBM) and C60 were purchased from American Dye Source and used as received. C60 SDS was synthesized by an augment procedure by Cataldo *et al.*.[26] The C60 SDS synthetic details are found in the supplemental information (SI). RWPt-1, 2 and 3 were prepared by previous literature procedures.[24-25]

All Ultraviolet Visible spectra were collected on an Agilent 8453 Spectrometer. Singlet oxygen emission spectra were collected on an Edinburgh Instruments FLS980 spectrometer whose details may be found from the manufacturer. A brief description may be found in the SI. The NMR spectra were collected on a Bruker Avance III Solution 300 spectrometer. All solution 1H spectra were referenced internally to tetramethylsilane and 13C spectra were referenced internally to chloroform. The femtosecond transient absorption experiments were collected on a Newport TAS. A description of the Newport TAS may be found in the SI. The nanosecond flash photolysis was collected on an Edinburgh Instruments LP980. A description of the Edinburgh LP980 is found in the SI.

RESULTS AND DISCUSSION

Structure and Electrochemistry. Shown in Scheme 1 are the molecular structures of platinum-containing "roller wheels", namely **RWPt-1**, **RWPt-2**, and **RWPt-3**. Also shown in Scheme 1 are the fullerene acceptors PCBM, C60 and C60 SDS used for quenching of the platinum-bisacetylide donor excited state.

Scheme 1. Chemical structures of RWPt complexes as well as fullerene derivatives utilized in this study.

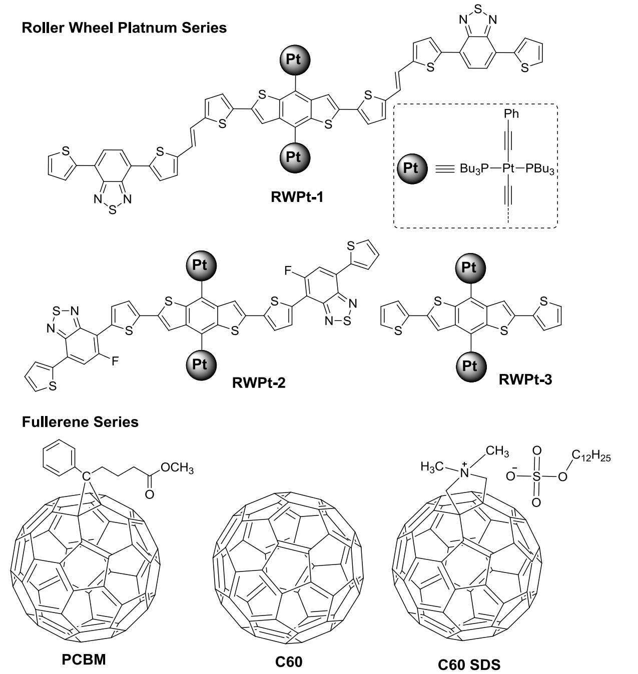

Each RWPt molecular structure features a Pt-bisacetylide benzenedithiophene as the electron rich core and an electron poor benzothiadiazole as the acceptor. The crystallinity or intermolecular packing of the RWPt molecular platform changes with the size of the acceptor as noted in the slip stack packing of **RWPt-1** from the single crystal XRD unit cell. While a single crystal XRD structure was unable to be obtained for **RWPt-2**, this slip stack packing is inferred from similarities with **RWPt-1** and its well-resolved powder XRD pattern.[24-25] As **RWPt-3** has an acceptor length of 0, no slip stack packing is observed in the single crystal XRD structure.[24]

As mentioned above, the series of quenchers utilized in this study are fullerenes with decreasing LUMO level from PCBM, C60, and a cationic C60 (SDS anion). Cyclic Voltammetry (CV) was performed on the platinum-bisacetylide RWPt compounds to measure the oxidation and reduction potentials, which may provide a rough estimate of the singlet HOMO and LUMO energies. Further, as triplet state energy approximations are unable to be observed by CV, TDDFT estimates of each complex are used to find triplet state potentials relative to the ground state potentials measured by CV. Likewise, CV was performed on the fullerenes to approximate the LUMO energies in order to predict possible quenchers for the RWPt triplet states. All HOMO and LUMO levels are measured at the oxidation and reduction onset potentials. The singlet HOMO and LUMO energies against vacuum are approximated by $E_{HOMO} = -(E_{ox} + 4.8)$ and $E_{LUMO} = -(E_{red} + 4.8)$, where the scalar 4.8 is relative to the external standard of Fc/Fc^+ in dicloromethane. From the CV data, the approximate HOMO and LUMO are −4.9, and −3.2 for **RWPt-1** and −5.0, and −3.2 eV for **RWPt-2**. The HOMO and LUMO energies for the **RWPt-3** model complex are −5.4 and −3.1 eV. TDDFT was previously utilized to estimate the triplet energies for **RWPt-1**, **-2** and **-3** to be −3.84, −3.88 and −3.5 eV.[25] CV performed on the series of fullerene acceptors approximates the LUMO energies to be -

3.77 (PCBM), -3.86 (C60) and -3.94 (C60SDS). The CV scans for the RWPt molecules and fullerenes are found in the supplemental information (SI1 and 2).[25]

Excited State Dynamics. The photoinduced excited state dynamics of the RWPt compounds is characterized by transient absorption (TA) from the femtosecond to the microsecond timescale. Depicted in Figure 1 are the stacked ground state electronic absorbance spectra (A) and TA spectra (B, C, D) over many orders of magnitude time delay for **RWPt-3**. For ease of interpretation, a bold black line at 0 OD is added to all TA figures and the data near the laser line have been removed. All single wavelength and global fitting kinetics are found in the supplemental (Section S4). All TA kinetic fitting for RWPt compounds are fit with the multi-exponential function (equation 1):

$$\Delta OD = e^{-(t/\tau_\rho)} + \sum_i A_i\, e^{-(t/\tau_i)} + A_{inf} e^{-(t/\tau_{inf})},$$
$$\tau_\rho = (IRF/2ln2)$$

Equation 1

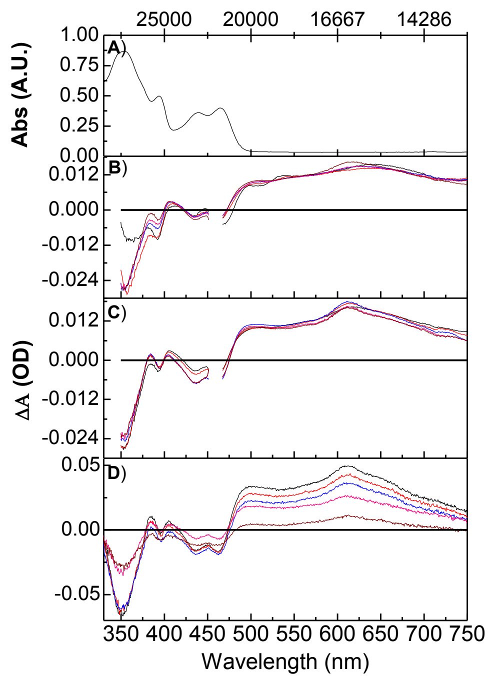

Figure 1 A) Absorbance Spectrum for RWPt-3. B) Ultrafast pump probe transients collected at 0.5 ps (black), 1 ps (red), 5 ps (blue), 10 ps (pink) and 25 ps (brown) time delays. C) Ultrafast pump probe transients collected at 25 ps (black), 50 ps (red), 1 ns (blue), 5 ns (pink), 7.4 ns (brown). D) Nanosecond flash photolysis transients collected at 30 ns (black), 6 μs (red), 10 μs (blue), 30 μs (pink), 50 μs (brown).

The ground state electronic absorbance spectrum of **RWPt-3** (Figure 1A) shows four pronounced electronic transitions at 352, 394, 439, and 465 nm. These transitions are assigned to individual BDT $\pi\rightarrow\pi^*$ transitions, based on time dependent density functional theory (TDDFT).[25] The ultrafast pump probe transient spectra of **RWPt-3** (Figure 1 B and C) feature two negative peaks or "bleaches" from 350 to 402 nm and 424 to 473 nm as well as two positive peaks or excited state absorptions from 402 to 424 nm and 473 to 750 nm. The nanosecond flash photolysis transient spectra (Figure 1D) feature the relaxation of the same bleach and excited state absorption peaks as the ultrafast pump probe experiment. Four kinetic time constants were extracted from the kinetic fitting of **RWPt-3** transient dynamics (Table1).

The assignments and discussion of **RWPt-3** excited state evolution are as follows. The global fitting analysis reveals time constants of 32 ps and 3660 ps for the femtosecond pump probe measurement and of 21560 ns and 63500 ns for the nanosecond flash photolysis. We have previously assigned τ_3 (21560 ns) and τ_4 (63500) to the electron hole recombination and a photodecomposition reaction, respectively.[24] The assignment of τ_2 (~3660 ps) is more difficult, as no major spectral changes are observed with the time constant. Thus, we tentatively assign this kinetic component to internal conversion. We find it unlikely that slow solvent reorganization is responsible for this kinetic component, though we cannot rule this out at present. We also acknowledge that internal conversion within the triplet manifold is generally fast, yet in this case we believe that coupling between different triplet states is weak. The first time constant (τ_1) of 32 ps is assigned to platinum assisted intersystem crossing from the single to triplet manifold. This assignment is predominantly based on the observation of isosbestic points at 525, 566 and 664 nm and that the state formed after this evolution has the same spectral features as the nanosecond flash photolysis spectra, which we have assigned as the excited triplet state. Furthermore, it is not uncommon to have fast intersystem crossing in organic molecules where the spin orbit coupling of heavy atoms is mixed with the $\pi\rightarrow\pi^*$ transition.[27]

Depicted in Figure 2 are the stacked ground state electronic absorbance spectra (A) and transient absorption data (B, C, D, E) for **RWPt-1** (Kinetic data found Supplemental S5). The global fitting results are found in Table 1.

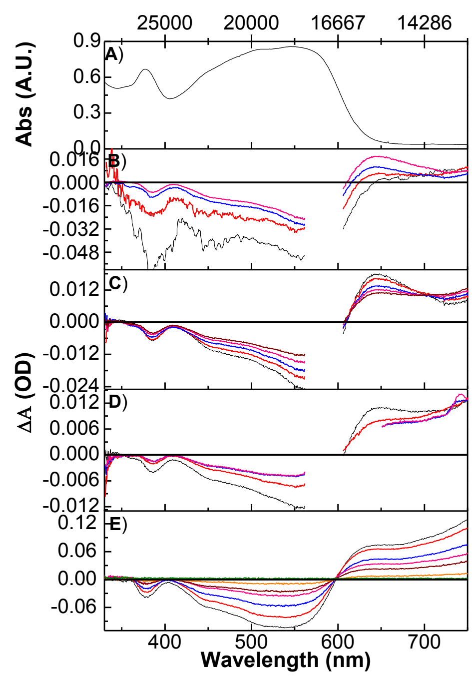

Figure 2 A) Absorbance Spectra for RWPt-1. B) TA spectra collected at 0.5 ps (black), 1 ps (red), 5 ps (blue) and 50 ps (pink) time delays. C) TA spectra collected at 50 ps (black), 250 ps (red), 500 ps (blue), 750 ps (pink) and, 1 ns (brown). D) TA spectra collected at 1 ns (black), 2.5 ns (red), 5 ns (blue) and 7.2 ns (pink). E) TA spectra collected at 30 ns

(black), 1 μs (red), 3 μs (blue), 5 μs (pink), 7 μs (brown), 12.5 μs (yellow) and, 37.5 μs (green).

The ground state electronic absorbance spectrum of **RWPt-1** (Figure 2A) features electronic transitions at 377 and 553 nm with a shoulder at ~450 nm. The broad absorption from 450 to 650 nm is a Pt-bisacetylide benzenedithiophene to benzothiadiazole charge transfer transition, and is distinct from that observed for **RWPt-3**. The peaks at 373 as well as the shoulder around 445 nm are thought to be from Pt-bisacetylide benzenedithiophene $\pi \rightarrow \pi^*$ transitions as in **RWPt-3**.[16] The ultrafast pump probe transient spectra of **RWPt-1** are divided into three sections (Figure 2 B, C, and D) to highlight spectral changes corresponding to the time constants from the global fitting analysis. The early time transients (Figure 2B; 0.5 to 50 ps time delays) feature initial ground state bleach from 350 to 643 nm (mirroring the electronic absorption spectra) and a growing excited state absorption from 611 to 750 nm. The intermediate transients (Figure 2C; 50 ps to 1000 ps time delay) feature the same ground state bleach and a developed excited state absorption from 610 to 750 nm. Two isosbestic points are observed in these transients at 615 and 706 nm. The late time pump probe transients (Figure 2D; 1ns to 7.2 ns time delay) feature loss of intensity in the long wavelength absorption and short wavelength bleach. No isosbestic points are observed in these transient spectra. The nanosecond flash photolysis transient spectra (Figure 2E) feature clear relaxation of ground state bleach and induced excited state absorption observed in the ultrafast pump probe experiment. A single isosbestic point is observed at 597 nm.

Four time constants are observed from the global kinetic fitting of the ultrafast pump probe and nanosecond flash photolysis transient kinetics for **RWPt-1**. Time constants of 0.3 ± 0.1, 5 ± 1 and 1070 ± 210 ps describe the ultrafast response, and a time constant of 5030 ± 60 ns characterizes the nanosecond data. Again these values are consistent with single wavelength kinetic fitting. The 5030 ± 60 ns time constant is ascribed to the electron hole recombination as a single time constant is observed for both the loss of the triplet excited state as the recovery of the ground state with a clear isosbestic point.[25] Working backwards in time from the nanosecond flash photolysis data, we ascribe the third time constant from the pump probe data (τ_3) of 1070 ± 210 ps to intersystem crossing from the singlet to triplet manifold. This assignment is supported by the similarity of the spectra observed at 7.2 ns and 30 ns. We next ascribe the 0.3 ± 0.01 ps time constant (τ_1) to relaxation of a vibrationally hot excited state. This assignment is primarily based on the observation of an intense ground state bleach in the absence of an excited state absorption signature in the 0.5 ps and 1 ps spectra. The second time constant (τ_2) of 5 ± 1 ps is thus assigned to the formation of the thermalized singlet excited state. This assignment is predicated on the observation of a new excited state feature at 645 nm, which is typically where singlet excited states are observed in these types of compounds.[13]

Depicted in Figure 3 are the ground state electronic absorbance spectra (A) and TA (B, C, D, E) for **RWPt-2**. The spectral transitions and temporal response of **RWPt-2** shares features with both **RWPt-1** and **RWPt-3**. Similar to **RWPt-3**, the ground state electronic absorbance spectrum of **RWPt-2** (Figure 3A) exhibits four pronounced electronic transitions at 363, 441, 490 and 570 nm, which are broader and shifted to longer wavelengths reminiscent of **RWPt-1**. The broad absorption from 500 to 650 nm is a Pt-bisacetylide benzenedithiophene to benzothiadiazole charge transfer transition.

Table 1 Global fitting kinetics for RWPt compounds and RWPt compounds with fullerene quenchers.

	RWPt-1	RWPt-1 + 5eq PCBM	RWPt-1 + 5eq C60	RWPt-1 + 5eq C60 SDS	RWPt-2	RWPt-2 + 5eq PCBM	RWPt-2 + 5eq C60	RWPt-2 + 10eq C60	RWPt-2 + 5eq C60SDS	RWPt-2 + 10eq C60SDS	RWPt-3
τ_1 (ps)	0.3 ± 0.1				0.3 ± 0.18						
τ_2 (ps)	5 ± 1				9 ± 4						32 ± 11
τ_3 (ps)	1070 ± 210				560 ± 60						3660 ± 1280
τ_4 (ns)	5030 ± 60	4770 ± 180	5090 ± 60	5030 ± 60	6080 ± 440	6300 ± 420	5990 ± 1420	3140 ± 20	4250 ± 2100		
τ_5 (ns)					14130 ± 170	16500 ± 430	12500 ± 430	12830 ± 250	9670 ± 740	7150 ± 10	21560 ± 4500

The peaks at 363, 441, and 490 nm are thought to be from Pt-bisacetylide benzenedithiophene $\pi \rightarrow \pi^*$ transitions as seen in RWPt-3.[16] Again, the TA single wavelength and global fitting kinetics are found in the SI (Supplemental section S6), and the global fitting results are displayed in Table 1.

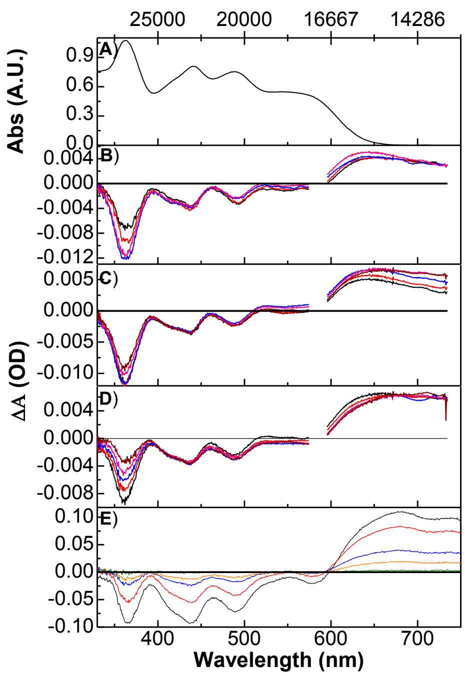

Figure 3 A) Absorbance Spectra for RWPt-2. B) TA spectra collected at 0.38 ps (black), 0.5 ps (red), 1 ps (blue) and 2.5 ps (pink) time delays. C) TA spectra collected at 2.5 ps (black), 5 ps (red), 25 ps (blue), 150 ps (pink) and, 250 ps (brown). D) TA spectra collected at 250 ps (black), 500 ps (red), 750 ps (blue), 1 ns (pink) and 7.2ns (brown). E) TA spectra collected at 30 ns (black), 5 μs (red), 15 μs (blue), 25 μs (orange) and, 55 μs (green).

The early time pump probe transients (Figure 3B; 0.4 to 2.5 ps time delay) of **RWPt-2** feature an initial ground state bleach from 350 to 600 nm that grows in intensity over this time interval (575 to 594 nm are omitted due to the presence of the laser line), and the emergence of an excited state absorption from 600 to 750 nm. The intermediate transients (Figure 3C; 2.5 to 250 ps time delay) show little change in the bleach region, but the excited state absorption from 515 to 750 nm increases in intensity and broadens to the red. In the late transients (Figure 3D; 250 to 7200 ps), the bleach decreases significantly in intensity, while the excited state absorption shows very little (ΔOD< 0.0005) change over this time regime. The nanosecond flash photolysis transient spectra (Figure 3E) display clear evidence of relaxation to the ground state complex. A single isosbestic point is observed at 598 nm.

The early time pump probe transients (Figure 3B; 0.4 to 2.5 ps time delay) of **RWPt-2** feature an initial ground state bleach from 350 to 600 nm that grows in intensity over this time interval (575 to 594 nm are omitted due to the presence of the laser line), and the emergence of an excited state absorption from 600 to 750 nm. The intermediate transients (Figure 3C; 2.5 to 250 ps time delay) show little change in the bleach region, but the excited state absorption from 515 to 750 nm increases in intensity and broadens to the red. In the late transients (Figure 3D; 250 to 7200 ps), the bleach decreases significantly in intensity, while the excited state absorption shows very little (ΔOD< 0.0005) change over this time regime. The nanosecond flash photolysis transient spectra (Figure 3E) display clear evidence of relaxation to the ground state complex. A single isosbestic point is observed at 598 nm.

The analysis and assignment of the TA kinetics for **RWPt-2** are more complex than for the **RWPt-1** and **RWPt-3** complex, as **RWPt-2** exhibits components from **RWPt-1** and **RWPt-3**. Throughout the entire time range, time constants of 0.3 ± 0.18 ps, 9 ± 4 ps, 560 ± 60 ps, 6080 ± 440 ns and 14130 ± 170 ns were retrieved from kinetic analysis. The first time component (τ_1) is assigned to vibrational cooling of the initially formed singlet excited state. The second time component (τ_2) in **RWPt-2** is assigned to the formation of the thermally relaxed S_n state similar to the **RWPt-1** complex. The assignment of τ_3 in the **RWPt-2** complex is to the formation of two orthogonal triplet excited states. For **RWPt-2**, two states need to be formed in order to understand the nanosecond flash photolysis data (see *Quenching* below). Interestingly, the observed time constant in **RWPt-2** is in between that of **RWPt-3** and **RWPt-1**, indicating that the two orthogonal excited state most likely resemble independent **RWPt-3** and **RWPt-1** moieties. As stated above we have previously assigned τ_4 and τ_5 as the electron hole recombination for the two orthogonal triplet excited states. The observation of two independent non-interacting triplet states is not common in organometallic polymers or small molecules, though it may help explain why bulk heterojunction devices made with **RWPt-2** performed better that **RWPt-3** and **RWPt-1**. As we will demonstrate bellow, these independent triplet states are not isoenergetic as quenching differences are observed with different fullerene acceptors. It is these differences that prompt the assignment of two independent triplet states.

Triplet Quenching with Fullerenes and $^3O_2$. In order to develop better photovoltaic or light emitting materials it is important to know the relative energy of the lowest lying triplet state in RWPt compounds. Phosphorescence has only been observed for **RWPt-3** to yield a direct measurement of the triplet energy of 1.76 eV. We have previously approximated the triplet energies in the **RWPt-1** and **RWPt-2** compounds by utilizing a combination of electrochemistry and TDDFT.[25] These experiments have enabled us to make predictions on the energy of quenchers required to quench each of the triplet states. The predictions are as follows: PCBM is predicted to only quench the singlet state of **RWPt-1** and **RWPt-2**. C60 is predicted to quench the singlet state of **RWPt 1** and **RWPt-2** as well as the two triplets of **RWPt-2**, but not the triplet of **RWPt-1**. C60 SDS is predicted to quench all of the excited state singlets and triplets in the RWPt complexes.

An experimental method of testing our predictions of the triplet state energies is by using quenchers as an upper and lower bracket for calculating the triplet energy. By this lifetime quenching method, we observe a partial breakdown of the CV and TDDFT approximations. The primary reason for the breakdown in our prediction originates from CV, which can only accurately predict energy levels upon an observation of a fully reversible couple. It is well known that irreversible reactions shift observed potential onsets and peak potentials in the CV experiment. The oxidation and reduction couples for RWPt compounds as well as other doped OPVs are often irreversible.

Shown in Figure 4 is the quenching of the two **RWPt-2** triplet states using our series of fullerenes. All normalized single wavelength kinetic traces were taken at 700 nm with the pure **RWPt-2** trace plotted first followed by addition of each fullerene.

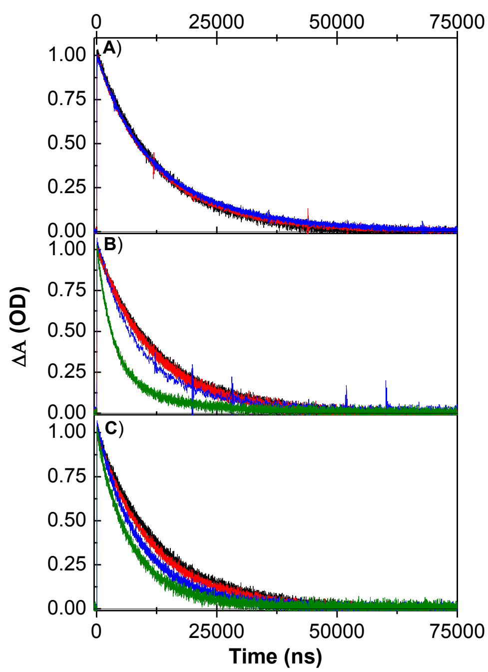

Figure 4 A) Single wavelength kinetics of RWPt-2 (black), RWPt-2 with 1 eq of PCBM (red), and with 5 eq of PCBM (blue). B) Single wavelength kinetics of RWPt-2 (black), RWPt-2 with 1 eq of C60 (red), RWPt-2 with 5 eq of C60 (blue) and, RWPt-2 with 10 eq of C60 (green). C) Single wavelength kinetics of RWPt-2 (black), RWPt-2 with 1 eq of C60 SDS (red), RWPt-2 with 5 eq of C60 SDS (blue) and, RWPt-2 with 10 eq of C60 SDS (green).

As expected, no quenching of the triplet state are observed upon addition of PCBM to **RWPt-2** as shown in Figure 4a. As predicted, the C60SDS fullerene quenches both triplet states in **RWPt-2** (Figure 4c). A Stern-Volmer (SV) analysis was applied to **RWPt-2** with C60 SDS fullerene. For SV analysis, low quencher concentrations are utilized to avoid quencher aggregation in chlorobenzene. Equation 2 is the formulation of the SV analysis where τ_0 is the unquenched donor lifetime, τ is the donor lifetime with a quencher and, Q is the quencher concentration.

$$\frac{\tau_0}{\tau} = 1 + (k_q\tau_0)[Q]$$

Equation 2.

Figure 5 is the Stern-Volmer plot for the **RWPt-2** donor with the C60 SDS fullerene. From the SV analysis, we see that the quenching has linear dependence with a quenching rate constant (k_q) of 3.7 x 10^9 M^{-1} s^{-1}.

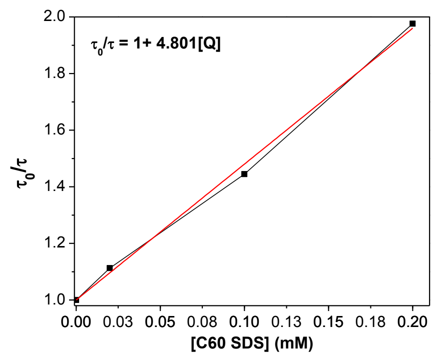

Figure 5 Stern-Volmer plot for RWPt-2 C60SDS solutions. The data points are taken from τ5 time component of the global fitting analysis. Error bars have been omitted. Lines connecting the data points have been added to help visualize the linear trend.

The breakdown of the CV approximations begins with the C60 where we observe quenching of only one of the two triplet states (Figure 4b). That only one of the lifetimes experiences quenching supports our earlier assignment of two independent triplet states. Global fitting of the flash photolysis kinetics yields a change in τ_4 from 6080 ± 440 μs to 3140 ± 20 μs at 10 eq without exhibiting a large change in μ_5 from 14130 ± 170 μs to 12800 ± 250 μs. One possible explanation for the lack of τ_5 quenching by C60 could be ascribed to a low driving potential between this triplet excited state and the C60 LUMO energy. The same SV analysis was performed for the quenching of the **RWPt-2** donor τ_4 with the C60 fullerene to yield a k_q of 1.6 x 10^9 M^{-1} s^{-1}. It should be mentioned that our k_q values are similar to those reported for the "dumbbell" type platinum-acetylide system(s) quenched with fullerenes.[22]

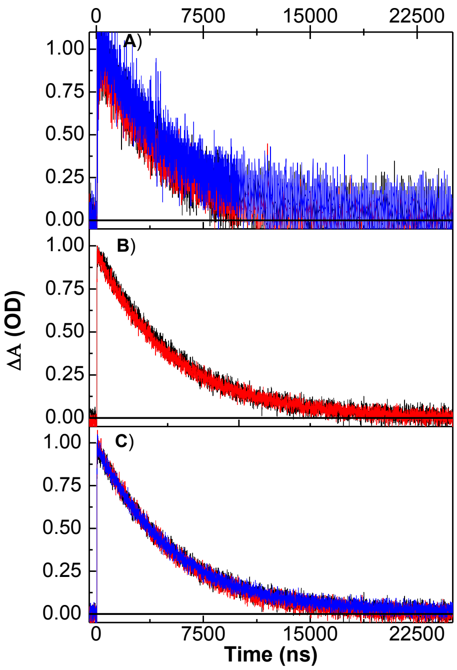

Figure 6 A) Single wavelength kinetics of RWPt-1 (black), RWPt-1 with 1 eq of PCBM (red) and, RWPt-1 with 5 eq of PCBM (blue). B) Single wavelength kinetics of RWPt-1 (black) and RWPt-1 with 5 eq of C60 (red) C) Single wavelength kinetics of RWPt-1 (black), RWPt-1 with 1 eq of C60 SDS (red) and, RWPt-1 with 5 eq of C60 SDS (blue).

The breakdown in the reduction potential estimates continues with the quenching of **RWPt-1** complex. Shown in Figure 6 is the quenching of the triplet state of **RWPt-1** using the series of fullerenes. All normalized single wavelength kinetic traces were taken at 780 nm with **RWPt-1** in the absence of quencher trace plotted first followed by addition of each fullerene. As predicted by the CV and TDDFT, PCBM and C60 do not quench the triplet state in **RWPt-1**. An unexpected result is that C60 SDS does not exhibit any quenching of the **RWPt-1** triplet state. While the exact reason for the lack of observed quenching with C60 SDS fullerene is not known, one explanation is that the real energy of the **RWPt-1** triplet state may be at least 100 mV less positive than the electrochemistry and computational predictions.

The final quencher utilized to better understand the energy of the triplet state is triplet oxygen. The singlet triplet gap in oxygen is at ~1 eV and thus should quench all of the triplet excited states of the RWPt compounds. Nanosecond flash photolysis and near-infrared emission experiments were collected on aerated RWPt solutions to measure singlet oxygen quenching. Shown in Figure 7 are global fitting kinetics for the triplet absorption of the aerated RWPt complexes.

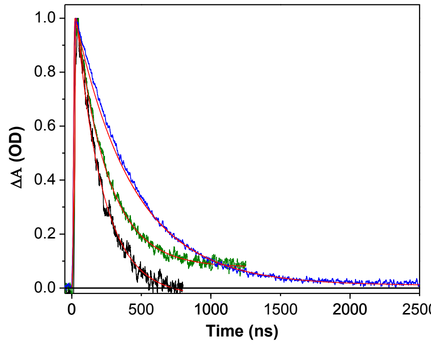

Figure 7 Global fitting kinetics of aerated RWPt complexes with RWPt-1 (black), RWPt-2 (green), and RWPt-3 (blue). Monoexponential fitting of the lifetimes are in red.

In Figure 7 we observe that the triplet lifetime of the three RWPt complexes is drastically shortened by the presence of oxygen. The decrease in lifetime is directly correlated to the appearance of $^1O_2$ emission in NIR emission experiments (Figure S 19). With the aerated solution lifetimes, the quenching rate was found to be 1.8 x 10^{10} M^{-1} s^{-1}, 1.9 x 10^{10} M^{-1} s^{-1}, and 3.2 x 10^{10} M^{-1} s^{-1} for **RWPt-1**, **RWPt-2**, and **RWPt-3**, respectively. From the $^1O_2$ emission intensities, the $^1O_2$ quantum yields were calculated by equation 3.

$$\phi_\Delta = \left(\frac{I}{A}\right) \times \left(\frac{A_{ref}}{I_{ref}}\right) \times \left(\frac{\tau_{\Delta\,ref}}{\tau_\Delta}\right) \times \phi_{\Delta\,ref}$$

Equation 3.

Where I is the integrated emission, A is the absorbance, τ_Δ is the $^1O_2$ lifetime which is solvent dependent and ϕ_Δ is the $^1O_2$ quantum yield. The calculated Φ_Δ are 0.30, 0.65, 1.49 for **RWPt-1**, **RWPt-2**, and **RWPt-3**, respectively. This decrease in excited state lifetime as well as $^1O_2$ emission suggests that the lowest triplet energy of the RWPt compounds is higher than 1 eV. We are surprised by Φ_Δ = 1.49 for **RWPt-3**, especially given the dilute solutions employed in these studies (see SI). A Φ_Δ > 1 is suggestive of a singlet fission mechanism in these materials. Calculations by Michl and coworkers have identified the slip stack semi-crystalline and crystalline morphology may be the preferred orbital geometry for singlet fission in organic materials.[28] As slip stack packing is observed in crystals of **RWPt-1** and two orthogonal triplets are observed in of **RWPt-2**, we do not rule out single fission type mechanisms though we will leave this discussion for future work.

From the sum of quenching experiments, it is now possible to experimentally comment on the triplet energies (relative to vacuum) in RWPt compounds. We estimate the triplet state energy of **RWPt-3** to be at -3.64 eV (relative to vacuum), directly from the emission spectra. The two triplet state energies in **RWPt-2** are between -3.77 and -3.86 for one triplet as well as -3.86 and -3.94 eV for the other triplet. The triplet state in **RWPt-1** is between -3.94 and -3.8 eV. These data are consistent with previous TD-DFT predictions that the S_0 to T_1 energy gap in **RWPT-1** and **RWPT-2** are 1.06 eV and 1.12 eV, respectively.

CONCLUSION

In conclusion, this study yields important insights of the structure function relationship for the formation of the triplet excited state as well as excited state energy of the lowest energy excited triplet states to be captured in a device application. We have also demonstrated capture as well as the need for the in-depth photophysical studies of organic donor-acceptor architectures as a partial breakdown of electrochemical and computational approximations commonly employed to select acceptors is observed. We note that for further work, the triplet energy of the RWPt compound will need to be raised in order to have at least 100 mV of driving force to the acceptor or a non-fullerene acceptor will need to be utilized with a LUMO energy < 3.7 eV (verses vacuum). In addition to excited state dynamics and triplet energies, an interesting discovery is made in relation to possible singlet fission in RWPt compounds. **RWPt-2** and possibly **RWPt-3** are thought to make multiple orthogonal triplet states as demonstrated by separate triplet quenching or greater that 100% singlet oxygen yield. While these molecules are capable of making a bulk heterojunction solar cell with a fullerene acceptor with 6% efficiency, it may be better to focus on a different solar cell design by mixing the RWPt compounds over a low band gap semiconductor in order to take advantage of the singlets and triplets generate by these molecules.

ASSOCIATED CONTENT

Supporting Information. Synthetic Details for C60 SDS, Full description of instrumentation, Cyclic Voltammetry of Fullerenes and RWPt moiety, Single Wavelength and Global Fitting Kinetics for RWPt -1,-2 and -3, Single Wavelength and Global Fitting Kinetics for RWPt-1 with PCBM, C60 and C60 SDS, Single Wavelength and Global Fitting Kinetics for RWPt-2 with PCBM, C60 and C60 SDS, $^1O_2$ emission and parameters.

AUTHOR INFORMATION

Corresponding Author

* J.J.R. E-mail: jrack@unm.edu

* Y.Q. E-mail: yangqin@unm.edu

NOTES

The authors declare no competing financial interest.

ACKNOWLEDGMENT

Y.Q. would like to acknowledge NSF (DMR-1453083) for financial support for this research. NM EPSCoR (NSF Grant No. IIA-1301346) and USDA (NIFA 2015-38422-24059) are acknowledged for partially supporting the research. JJR acknowledges NSF (Grant CHE 1602240) for financial support.

REFERENCES

(1) Wu, Z.; Ma, D. Recent Advances in White Organic Light-Emitting Diodes. *Mat. Sci. Eng. R.* **2016,** *107*, 1-42,

(2) Lu, L. Y.; Zheng, T. Y.; Wu, Q. H.; Schneider, A. M.; Zhao, D. L.; Yu, L. P. Recent Advances in Bulk Heterojunction Polymer Solar Cells. *Chem. Rev.* **2015,** *115* (23), 12666-12731,

(3) Chen, Y.; Wan, X.; Long, G. High Performance Photovoltaic Applications Using Solution-Processed Small Molecules. *Acc. Chem. Res.* **2013,** *46* (11), 2645-2655,

(4) Roncali, J.; Leriche, P.; Blanchard, P. Molecular Materials for Organic Photovoltaics: Small is Beautiful. *Adv. Mater.* **2014,** *26* (23), 3821-3838,

(5) Thompson, B. C.; Fréchet, J. M. J. Polymer–Fullerene Composite Solar Cells. *Angew. Chem. Int. Ed.* **2008,** *47* (1), 58-77,

(6) Mikhnenko, O. V.; Blom, P. W. M.; Nguyen, T.-Q. Exciton Diffusion in Organic Semiconductors. *Energy Environ. Sci.* **2015,** *8* (7), 1867-1888,

(7) Mikhnenko, O. V.; Azimi, H.; Scharber, M.; Morana, M.; Blom, P. W. M.; Loi, M. A. Exciton Diffusion Length in Narrow Bandgap Polymers. *Energy Environ. Sci.* **2012,** *5* (5), 6960-6965,

(8) Castrucci, J. S.; Josey, D. S.; Thibau, E.; Lu, Z.-H.; Bender, T. P. Boron Subphthalocyanines as Triplet Harvesting Materials within Organic Photovoltaics. *J. Phys. Chem. Lett.* **2015,** *6* (15), 3121-3125,

(9) Luppi, B. T.; Majak, D.; Gupta, M.; Rivard, E.; Shankar, K. Triplet Excitons: Improving Exciton Diffusion Length for Enhanced Organic Photovoltaics. *J. Mater. Chem. A* **2019,** *7* (6), 2445-2463,

(10) Rao, A.; Friend, R. H. Harnessing Singlet Exciton Fission to Break the Shockley–Queisser Limit. *Nat. Rev. Mater.* **2017,** *2*, 17063,

(11) Williams, R. M.; Chen, H.-C.; Di Nuzzo, D.; Meskers, S. C. J.; Janssen, R. A. J. Ultrafast Charge and Triplet State Formation in Diketopyrrolopyrrole Low Band Gap Polymer/Fullerene Blends: Influence of Nanoscale Morphology of Organic Photovoltaic Materials on Charge Recombination to the Triplet State. *J. Spectros.* **2017,** *2017*, 16,

(12) Cekli, S.; Winkel, R. W.; Alarousu, E.; Mohammed, O. F.; Schanze, K. S. Triplet Excited State Properties in Variable Gap π-Conjugated Donor-Acceptor-Donor Chromophores. *Chem. Sci.* **2016,** *7* (6), 3621-3631,

(13) Guo, F.; Ogawa, K.; Kim, Y.-G.; Danilov, E. O.; Castellano, F. N.; Reynolds, J. R.; Schanze, K. S. A Fulleropyrrolidine End-Capped Platinum-Acetylide Triad: the Mechanism of Photoinduced Charge Transfer in Organometallic Photovoltaic Cells. *Phys. Chem. Chem. Phys.* **2007,** *9* (21), 2724-2734,

(14) Chawdhury, N.; Köhler, A.; Friend, R. H.; Wong, W. Y.; Lewis, J.; Younus, M.; Raithby, P. R.; Corcoran, T. C.; Al-Mandhary, M. R. A.; Khan, M. S. Evolution of Lowest Singlet and Triplet Excited States with Number of Thienyl Rings in Platinum Poly-ynes. *J. Chem. Phys.* **1999,** *110* (10), 4963-4970,

(15) Kohler, A.; Wittmann, H. F.; Friend, R. H.; Khan, M. S.; Lewis, J. The Photovoltic Effect in a Platinum Poly-yne. *Synth. Met.* **1994,** *67* (1-3), 245-249,

(16) Wong, W.-Y.; Harvey, P. D. Recent Progress on the Photonic Properties of Conjugated Organometallic Polymers Built Upon the trans-Bis(para-ethynylbenzene)bis(phosphine)platinum(II) Chromophore and Related Derivatives. *Macromol. Rapid Commun.* **2010,** *31* (8), 671-713,

(17) Long, N. J.; Williams, C. K. Metal Alkynyl σ Complexes: Synthesis and Materials. *Angew. Chem. Int. Ed.* **2003,** *42* (23), 2586-2617,

(18) Harvey, P. D.; Gray, H. B. Low-lying Singlet and Triplet Electonic Excited States of Binuclear (D10-D10) Palladium and Platinum Complexes. *J. Am. Chem. Soc.* **1988,** *110* (7), 2145-2147,

(19) Juvenal, F.; Lei, H.; Schlachter, A.; Karsenti, P.-L.; Harvey, P. D. Ultrafast Photoinduced Electron Transfers in Platinum(II)-Anthraquinone Diimine Polymer/PCBM Films. *J. Phys. Chem. C* **2019,** *123* (9), 5289-5302,

(20) Wong, W.-Y.; Ho, C.-L. Di-, Oligo- and Polymetallaynes: Syntheses, Photophysics, Structures and Applications. *Coordin. Chem. Rev.* **2006,** *250* (19–20), 2627-2690,
(21) Mei, J.; Ogawa, K.; Kim, Y.-G.; Heston, N. C.; Arenas, D. J.; Nasrollahi, Z.; McCarley, T. D.; Tanner, D. B.; Reynolds, J. R.; Schanze, K. S. Low-Band-Gap Platinum Acetylide Polymers as Active Materials for Organic Solar Cells. *ACS Appl. Mater. Interfaces* **2009,** *1* (1), 150-161,
(22) Hsu, H.-Y.; Vella, J. H.; Myers, J. D.; Xue, J.; Schanze, K. S. Triplet Exciton Diffusion in Platinum Polyyne Films. *J. Phys. Chem. C* **2014,** *118* (42), 24282-24289,
(23) Chen, Z.; Hsu, H.-Y.; Arca, M.; Schanze, K. S. Triplet Energy Transport in Platinum-Acetylide Light Harvesting Arrays. *J. Phys. Chem. B* **2015,** *119* (24), 7198-7209,
(24) He, W.; Livshits, M. Y.; Dickie, D. A.; Yang, J.; Quinnett, R.; Rack, J. J.; Wu, Q.; Qin, Y. A "Roller-Wheel" Pt-Containing Small Molecule that Outperforms its Polymer Analogs in Organic Solar Cells. *Chem. Sci.* **2016,** *7* (9), 5798-5804,
(25) He, W.; Livshits, M. Y.; Dickie, D. A.; Zhang, Z.; Mejiaortega, L. E.; Rack, J. J.; Wu, Q.; Qin, Y. "Roller-Wheel"-Type Pt-Containing Small Molecules and the Impact of "Rollers" on Material Crystallinity, Electronic Properties, and Solar Cell Performance. *J. Am. Chem. Soc.* **2017,** *139* (40), 14109-14119,
(26) Cataldo, F.; Iglesias-Groth, S.; Manchado, A. On the Radical Anion Spectra of Fullerenes C60 and C70. *Fuller. Nanotub. Car. N.* **2013,** *21* (6), 537-548,
(27) Llewellyn, B. A.; Slater, A. G.; Goretzki, G.; Easun, T. L.; Sun, X.-Z.; Davies, E. S.; Argent, S. P.; Lewis, W.; Beeby, A.; George, M. W.; Champness, N. R. Photophysics and Electrochemistry of a Platinum-Acetylide Disubstituted Perylenediimide. *Dalton Trans.* **2014,** *43* (1), 85-94,
(28) Buchanan, E. A.; Michl, J. Packing Guidelines for Optimizing Singlet Fission Matrix Elements in Noncovalent Dimers. *J. Am. Chem. Soc.* **2017,** *139* (44), 15572-15575,

TOC Graphic

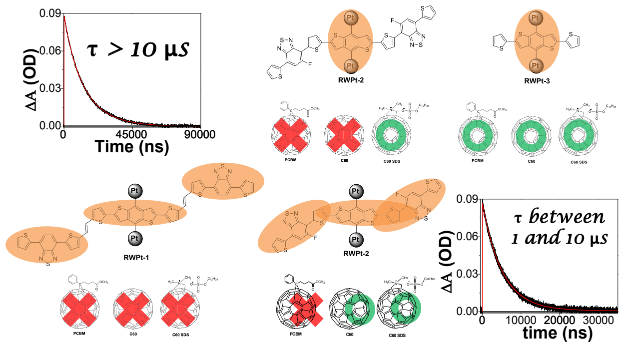
τ > 10 μs
ΔA (OD)
Time (ns)
RWPt-2
RWPt-3
RWPt-1
RWPt-2
τ between
1 and 10 μs
ΔA (OD)
time (ns)